its heat can be carried by conduction alone and in the absence of convection the dynamo ceases to exist[12,28,29]. Because of the high S content of the core and the low Fe–FeS eutectic temperature at the pressures applicable to Mars, it is possible that Mars has a totally liquid core at present with no inner core. In any case, radioactive heat generation by ^{40}K in the core of Mars should be considered in dynamo models for Mars and its ancient global magnetic field.

In conclusion, it definitely seems possible that radioactive heat due to ^{40}K can affect the thermal evolution and global processes in the Earth and Mars. Experimental verification using these techniques would enable us to determine whether U and Th are also potential contributors to radioactive heat in the cores of these planets. □

Methods

Dry polishing of samples

It has long been known that potassium sulphide is highly water-soluble, and previous studies have carefully avoided the use of water during polishing. As an alternative, water-free commercial lapping oils have been routinely employed in recent potassium partitioning experiments. We found that polishing in lapping oil causes significant, time-dependent, and variable loss of potassium from the metal sulphide phase, up to an order of magnitude, depending on how many polishing cycles are used. K is highly labile from the sulphide phase in such samples, and can be completely lost from the sulphide phase within a few hours of exposure to air after oil polish. Here we have developed a dry-polishing technique that avoids all liquids. Hexagonal boron nitride powder, which is nearly twice as lubricious as graphite, is used as a lubricant in the lapping operations. The boron nitride powders we used were Grade HCJ-48 (Union Carbide Corp.) for coarse polishing steps and Grade AC6003 (Advanced Ceramic Corp.) for below 12-μm level polishing. Boron nitride powder spread on carborundum papers allowed good hand polishing of the samples. Excellent polish down to 0.3 μm can be attained by this dry polishing technique and may be particularly useful in studies of distribution of alkali elements in high-pressure, high-temperature experiments.

High-pressure experiments

All experiments reported here used a double capsule technique in which the charge was loaded into an inner graphite capsule that was then sealed in a welded Pt outer capsule. Mass-balance calculations show no loss of K in these experiments, in contrast to those with single capsules. Experiments were conducted in an end-loaded piston cylinder apparatus. Temperatures were monitored using a tungsten-rhenium thermocouple (W5%Re/W26%Re) thermocouple, ignoring the effects of pressure on thermocouple electromotive force. Samples were analysed on the JEOL 8900 electron microprobe at the Geophysical Laboratory. All samples contained blebs of iron sulphide, up to 800 μm in diameter with small amounts (<4% vol.) of pure Fe blebs (<20 μm in diameter), surrounded by glassy silicate. Silicate glasses were analysed at 15 kV and 12 nA using a broad beam of approximately 15 μm in diameter to prevent K volatilization during analysis. Sulphides were analysed at 15 kV and 20 nA with a beam of 5 μm in diameter, using Si as a monitor for silicate contamination. Further analytical details and images of a representative sample are provided in the Supplementary Information.

Received 28 October 2002; accepted 7 March 2003; doi:10.1038/nature01560.

1. Lewis, J. S. Consequences of the presence of sulfur in the core of the Earth. *Earth Planet. Sci. Lett.* **11,** 130–134 (1971).
2. Hall, H. T. & Murthy, V. R. The early chemical history of the Earth: some critical elemental fractionations. *Earth Planet. Sci. Lett.* **11,** 239–244 (1971).
3. Oversby, V. M. & Ringwood, A. E. Potassium distribution between metal and silicate and its bearing on the occurrence of potassium in the Earth's core. *Earth Planet. Sci. Lett.* **14,** 345–347 (1972).
4. Goettel, K. A. Partitioning of potassium between silicates and sulphide melts: experiments relevant to the Earth's core. *Phys. Earth Planet. Inter.* **6,** 161–166 (1972).
5. Murrell, M. T. & Burnett, D. S. Partitioning of K, U, and Th between sulfide and silicate liquids: Implications for radioactive heating of planetary cores. *J. Geophys. Res.* **91,** 8126–8136 (1986).
6. Chabot, N. L. & Drake, M. J. Potassium solubility in metal: the effects of composition at 15 kbar and 1900 °C on partitioning between iron alloys and silicate melts. *Earth Planet. Sci. Lett.* **172,** 323–335 (1999).
7. Gessmann, C. K. & Wood, B. J. Potassium in the Earth's core? *Earth Planet. Sci. Lett.* **200,** 63–78 (2002).
8. Ohtani, E., Yurimoto, H. & Seto, S. Element partitioning between metallic liquid, silicate liquid, and lower-mantle minerals: implications for core formation of the Earth. *Phys. Earth Planet. Inter.* **100,** 97–114 (1997).
9. Gubbins, D., Masters, T. G. & Jacobs, J. A. Thermal evolution of the Earth's core. *Geophys. J. R. Astron. Soc.* **59,** 57–99 (1979).
10. Buffett, B. A., Huppert, H. E., Lister, J. R. & Woods, A. W. On the thermal evolution of the Earth's core. *J. Geophys. Res.* **101,** 7989–8006 (1996).
11. Labrosse, S., Poirier, J.-P. & Le Mouel, J.-L. The age of the inner core. *Earth Planet. Sci. Lett.* **190,** 111–123 (2001).
12. Stevenson, D. J., Spohn, T. & Schubert, G. Magnetism and thermal evolution of the terrestrial planets. *Icarus* **54,** 466–489 (1983).
13. Walter, M. J. & Thibault, Y. Partitioning of tungsten and molybdenum between metallic liquid and silicate melt. *Science* **270,** 1186–1189 (1995).
14. Jana, D. & Walker, D. The influence of silicate melt composition on distribution of siderophile elements among metal and silicate liquids. *Earth Planet. Sci. Lett.* **150,** 463–472 (1997).
15. Righter, K., Drake, M. J. & Yaxley, G. Prediction of siderophile element metal/silicate partition coefficients to 20 GPa and 2800 °C: the effects of pressure, temperature, oxygen fugacity, and silicate and metallic melt composition. *Phys. Earth Planet. Inter.* **100,** 115–134 (1997).
16. Righter, K. & Drake, M. J. Metal/silicate equilibrium in a homogeneously accreting Earth: New results for Re. *Earth Planet. Sci. Lett.* **146,** 541–554 (1997).
17. Gessmann, C. K. & Rubie, D. C. The origin of the depletions of V, Cr and Mn in the mantles of the Earth and Moon. *Earth Planet. Sci. Lett.* **184,** 95–107 (2000).
18. Li, J. & Agee, C. B. The effect of pressure, temperature, oxygen fugacity and composition on partitioning of nickel and cobalt between liquid Fe-Ni-S alloy and liquid silicate: Implications for the Earth's core formation. *Geochim. Cosmochim. Acta* **65,** 1821–1832 (2001).
19. Hillgren, V. J., Gessmann, C. K. & Li, J. in *Origin of the Earth and Moon* (eds Canup, R. M. & Righter, K.) 245–263 (Univ. Arizona Press, Tucson, 2000).
20. Holzheid, A. & Grove, T. L. Sulfur saturation limits in silicate melts and their implications for core formation scenarios for terrestrial planets. *Am. Mineral.* **87,** 227–237 (2002).
21. McDonough, W. F. & Sun, S.-S. The composition of the Earth. *Chem. Geol.* **120,** 223–253 (1995).
22. Buffett, B. A. Estimates of heat flow in the deep mantle based on the power requirements for the geodynamo. *Geophys. Res. Lett.* **29,** doi:10.1029/2001GL014649 (2002).
23. McKenzie, D. & Richter, F. M. Parameterized thermal convection in a layered region and the thermal history of the Earth. *J. Geophys. Res.* **86,** 11667–11680 (1981).
24. Bertka, C. M. & Fei, Y. Implications of Mars Pathfinder data for the accretion history of the terrestrial planets. *Science* **281,** 1838–1840 (1998).
25. Fei, Y., Li, J., Bertka, C. M. & Prewitt, C. T. Structure type and bulk modulus of Fe_3S, a new iron-sulfur compound. *Am. Mineral.* **85,** 1830–1833 (2000).
26. Lodders, K. & Fegley, B. An oxygen isotope model for the composition of Mars. *Icarus* **126,** 373–394 (1997).
27. Acuña, M. H. *et al.* Global distribution of crustal magnetization discovered by the Mars Global Surveyor MAG/ER experiment. *Science* **284,** 790–793 (1999).
28. Stevenson, D. J. Mars core and magnetism. *Nature* **412,** 214–219 (2001).
29. Nimmo, F. & Stevenson, D. J. The influence of early plate tectonics on the thermal evolution and magnetic field of Mars. *J. Geophys. Res.* **105,** 11969–11979 (2000).

Supplementary Information accompanies the paper on **www.nature.com/nature**.

Acknowledgements We thank M. Drake and D. Draper for comments and suggestions, N. Irvine for providing the K-silicate glass, B. Mysen for advice on silicate melt properties, C. Hadidiacos for assistance in electron microprobe analyses and C. Alexander, R. Carlson, E. Hauri, J. Li, F. Nimmo, D. Stevenson and J. Van Orman for discussions. This work was supported by a Grant-in-aid from the University of Minnesota (V.R.M.), the NASA (Y.F.), a Carnegie Institution Postdoctoral Fellowship and the Swiss National Science Foundation (W.v.W.).

Competing interests statement The authors declare that they have no competing financial interests.

Correspondence and requests for materials should be addressed to V.R.M. (vrmurthy@umn.edu).

Universal scaling relations in food webs

Diego Garlaschelli*†, Guido Caldarelli* & Luciano Pietronero*‡

** INFM UdR Roma 1 and Dipartimento di Fisica Università di Roma 'la Sapienza', P. le A. Moro 5, 00185 Rome, Italy*
† INFM UdR Siena and Dipartimento di Fisica Università di Siena, Via Roma 56, 53100 Siena, Italy
‡ CNR, Istituto di Acustica 'O.M. Corbino', v. Fosso del Cavaliere 100, 00133 Roma, Italy

The structure of ecological communities is usually represented by food webs[1–3]. In these webs, we describe species by means of vertices connected by links representing the predations. We can therefore study different webs by considering the shape (topology) of these networks[4,5]. Comparing food webs by searching for regularities is of fundamental importance, because universal patterns would reveal common principles underlying the organization of different ecosystems. However, features observed in small food webs[1–3,6] are different from those found in large ones[7–15]. Furthermore, food webs (except in isolated cases[16,17]) do not share[18,19] general features with other types of network (including the Internet, the World Wide Web and biological webs). These features are a small-world character[4,5] and a scale-free (power-law) distribution of the degree[4,5] (the number of

links per vertex). Here we propose to describe food webs as transportation networks[20] by extending to them the concept of allometric scaling[20–22] (how branching properties change with network size). We then decompose food webs in spanning trees and loop-forming links. We show that, whereas the number of loops varies significantly across real webs, spanning trees are characterized by universal scaling relations.

To analyse the statistical features of food webs, we propose to focus on their transportation properties[20]. This is possible because the directionality of the links (pointing from prey to predator[1]) defines a 'flow' of resources[1,23] (energy, nutrients and prey) between the vertices of the web. Here vertices are trophic species[12,24], defined as sets of biological species sharing the same predators and the same prey. Because every species feeds directly or indirectly on environmental resources to survive[1–3], food webs are connected (that is, every species can be reached by starting from an additional 'source' vertex representing the environment[23]). This allows us to define a spanning tree of a generic food web as a loopless subset of the links of the web such that, starting from the environment, every species can be reached by the flow (see Fig. 1). Hereafter, the term 'loop' indicates any closed path of links, ignoring the direction. A spanning tree of a web with S species (environment excluded) and L links has only S links. The remaining $L - S$ links are a measure of the number of loops in the whole web. For a given web, several spanning trees might exist. In Methods we discuss some possible criteria (chain length minimization and chain strength maximization) that allow the isolation of the minimal spanning tree, which is somehow related to the main transfer of resources in the webs. For reasons of brevity, we denote as 'strong' links the S links in the spanning tree and as 'weak' links the remaining $L - S$ ones.

Having reduced the complexity of the whole structure to a simpler tree, we can now study how the resources are delivered in the ecosystem. We then perform a typical analysis[20] introduced for other transportation networks such as river basins[20,25] and vascular systems[20–22]. This analysis consists of measuring the degree of optimization of the transfer rate. In more detail, for each species i in the spanning tree (the environment is labelled by $i = 0$), we compute the number A_i of species feeding directly or indirectly on i (plus species i itself). We also compute the sum $C_i = \sum_k A_k$, where k runs over the set of predators of i plus i itself (see Fig. 1b). Note that $A_0 = S + 1$, where S is the number of species (environment excluded). In both river[20] and vascular[21,22] networks, the shape of C_i as a function of A_i is universal (for every river and any living organism, respectively) and optimized. In Fig. 2a–g, we show the result (see Methods) of plotting C_i as a function of A_i (for each species $i = 0,S$) for the seven largest food webs in the literature, including (in order of increasing number of trophic species S) St Martin Island[7] ($S = 42$), St Marks seagrass[8] ($S = 48$), grassland[9] ($S = 63$), Silwood Park[10] ($S = 81$), Ythan Estuary without parasites[11] ($S = 81$), Little Rock Lake[12] ($S = 93$) and Ythan Estuary with parasites[13] ($S = 123$). Remarkably, in all food webs, we find a power-law scaling of the form $C \propto A^{\eta}$ with exponents in the range 1.13–1.16 (see Fig. 2a–g). These power-law relations are usually called allometric[20–22]. They describe how the topological properties scale with network size, and are related to the self-similarity[21,22,25] of the tree-like structure. In other words, they signal that the structure of the whole tree is statistically equivalent to that of any of its branches. Here, the observation of self-similarity is reinforced by the fact that source webs (for example, Silwood Park, reporting all the interactions based on the scotch broom *Cytisus scoparius*[10] and hence being a 'branch' of a larger, undocumented web) display the same scaling as the other webs. In a river network[25], where A_i is the area of the drainage basin of point i, the exponent is $\eta = 3/2$. This relation holds for any river (the exponent is universal) and hence suggests a common hydrogeological evolution[25]. For the vascular system[21,22] of an organism, there is no direct measure of the single values of A_i and C_i. Nevertheless, it is possible to relate the global quantities A_0 and C_0 to the metabolic rate B and to the body mass M, respectively, of the organism[20]. From Kleiber's empirical law[26], $B(M) \propto M^{3/4}$ (valid for several orders of magnitude of M), we have the relation $C_0 \propto (A_0)^{\eta}$ with $\eta = 4/3$. In this case, too, the universality of the exponent suggests that vascular systems of all organisms have been shaped by a common evolutionary process[22].

Similarly, the observation of universality in food webs would highlight common organizing principles across different ecosystems (despite the diversity[7–15] of the environments, ranging from terrestrial to aquatic, from desert to freshwater, and so on). We stress that, even in an ideal system, the correct scaling relations are expected to hold in the large-scale limit. Here, the largest webs have an exponent η of 1.13, whereas the smallest ones have higher exponents marginally consistent with 1.13. This indicates that $\eta = 1.13$ might represent the correct (universal) behaviour for large webs. To test this universality hypothesis, we select only the large-scale behaviour for each web. As with metabolic rates, we plot C_0 against A_0 (see Fig. 2h) for the seven webs together (see Methods) plus the webs of Coachella Valley[14] ($S = 29$), Skipwith Pond[15] ($S = 25$) and an average over the 181 webs of the EcoWeb database[6] (mean $S = 16$). This rather comprehensive analysis includes almost all published food webs; the numbers of species range from $S = 16$ to $S = 124$. Remarkably (see Fig. 2h), we find again a scaling relation fitted by the exponent $\eta = 1.13 \pm 0.03$, confirming the expectation of our universality hypothesis and indicating that the scaling might indeed be invariant across large food webs.

A quantitative comparison with other systems is again particularly revealing. In general, the value of the scaling exponent η measures the efficiency of resource transfer[20]. In a transportation system, A_i is proportional to the quantity of resources (water or blood) exchanged at point i, and C_i measures the 'cost' of this transfer[20]. Note that here we are referring to a 'global' notion of efficiency, measuring whether network topology optimizes the supply of resources to (or from) a given point (the outlet, the heart or the environment) from (or to) any other. This global efficiency should not be confused with the 'local' efficiency of a single-link transfer, which is always small[1–3], as discussed in Methods. Two independent proofs exist[20,22] that, for a tree-like network embedded in a space of euclidean dimension d, the exponent maximizing efficiency has the minimum value $\eta_{\mathrm{eff}} = (d + 1)/d$. At the opposite limit, the least efficient configuration (corresponding to a space-filling spiral or chain) yields the maximum value $\eta = 2$. This means that both river ($d = 2$) and vascular ($d = 3$) networks display an optimized degree of efficiency and suggests that their evolution shaped them to minimize the cost functions C_i. Our results show that the value of the exponent is smaller in food webs than in other systems. This is due to the absence of any euclidean dimension d (species are not constrained

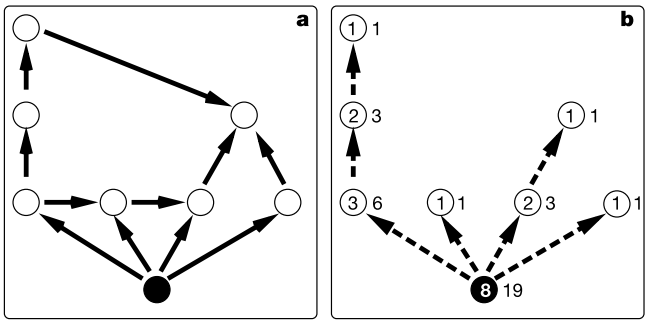

Figure 1 Computation of A_i and C_i from a spanning tree of the food web. **a**, Example of a food web with $S = 7$. The black vertex is the external environment. Species are layered in trophic levels. **b**, A possible spanning tree of the web. A_i is in the centre of each vertex i, C_i on the right. (See the text and Methods for details.)

to occupy the 'sites' of a regular lattice on a plane or in the space). In other words, spanning trees derived from food webs can in principle range between two extreme topologies: the chain-like (the least efficient, with all species feeding sequentially on one another, yielding $\eta = 2$ as before) and the star-like (the 'new' optimized state, with all species feeding directly on the environment, corresponding to the limit $\eta \to 1$) configuration. Remarkably, food web topology is more efficient than that of rivers or vascular systems; however, the optimal star-like configuration is not realized. This is related to the number of trophic levels[1] (the number of links in the shortest chains from the environment to the species; see Methods) in a food web: a tree spanning S species is chain-like if there are S distinct trophic levels, and star-like if there is only one level (which yields $C_i = A_i = 1$ for all $i = 1,S$ and $C_0 = 2A_0 - 1$, trivially corresponding to $\eta = 1$). As a result of competition, not every species can prey on the same resource. Species therefore tend to differentiate and occupy more than one trophic level to coexist[23]. However, empirical observations[1–3,6–15] reveal that real food webs display a small number of levels (usually in the range two to four) even if the number of species is large, which is consistent with our finding that η is closer to 1 than to 2.

We showed that the scaling exponent η is independent of other topological quantities, in particular the connectance $c = L/S^2$, which is the ratio of observed to possible links[12] (ranging from $c = 0.02$ in grassland to $c = 0.31$ in Skipwith Pond). Although a set of webs is consistent with the 'constant connectance' hypothesis[27] (according to which c is expected to be approximately constant about the value 0.1), two extreme deviations from this prediction are observed. The large values ($c = 0.31$) observed in Coachella Valley and Skipwith Pond are probably related to their small size[28]. In other webs, c seems to decrease as the fraction of parasitic links (from larger to smaller species) increases[9]: the addition of parasitic interactions[13] to the Ythan Estuary web[11] decreases c from 0.06 to 0.04. The simultaneous presence of predators, pathogens and parasites[10] in Silwood Park yields the intermediate value $c = 0.03$. Finally, grassland (describing almost only flows from a larger to smaller species[9]) has the smallest value $c = 0.02$, thus being very close to a tree-like structure. These results are consistent with Cousins's conjecture[29], which states that "the passage of energy from large to small organisms involves problems so great that the parasite has to specialize on a single species or single family of species". Our results suggest that these evolutionary constraints do not affect the shape of the spanning trees. This differs radically from the predictions of current food web models[3,23,24], where all topological features (including the form of the spanning tree) are tuned by the same parameter determining the connectance. As shown in Table 1, the Cascade[3] and Niche[24] (static) models fail to reproduce the values of c and η simultaneously for any real web. A dynamic model such as the Webworld[23–30] model (which describes evolving species in terms of a time-dependent set of features determining their interactions) succeeds in reproducing both quantities in its 'evolved' asymptotic state (see Table 1 and legend), but only for the webs consistent with the 'constant connectance' hypothesis. This occurs because, in the model, a species displaying a set of features can in principle evolve to display any other feature[23]. According to Cousins's conjecture, this possibility becomes unrealistic for parasitic interactions: being a specialized parasite of a certain host is likely to prevent specialization against other species.

Recent studies[28] relate the connectance to the stability of food webs. The robustness of real webs against successive removals of either a randomly chosen species or the most connected species increases monotonically[28] with c (which is thus a measure of the stability). In our framework, this means that the stability increases as the number of 'weak' links increases ('strong' links contribute only a negligible term $1/S$ to c). Our results then indicate that 'strong' and 'weak' links might have complementary roles: the

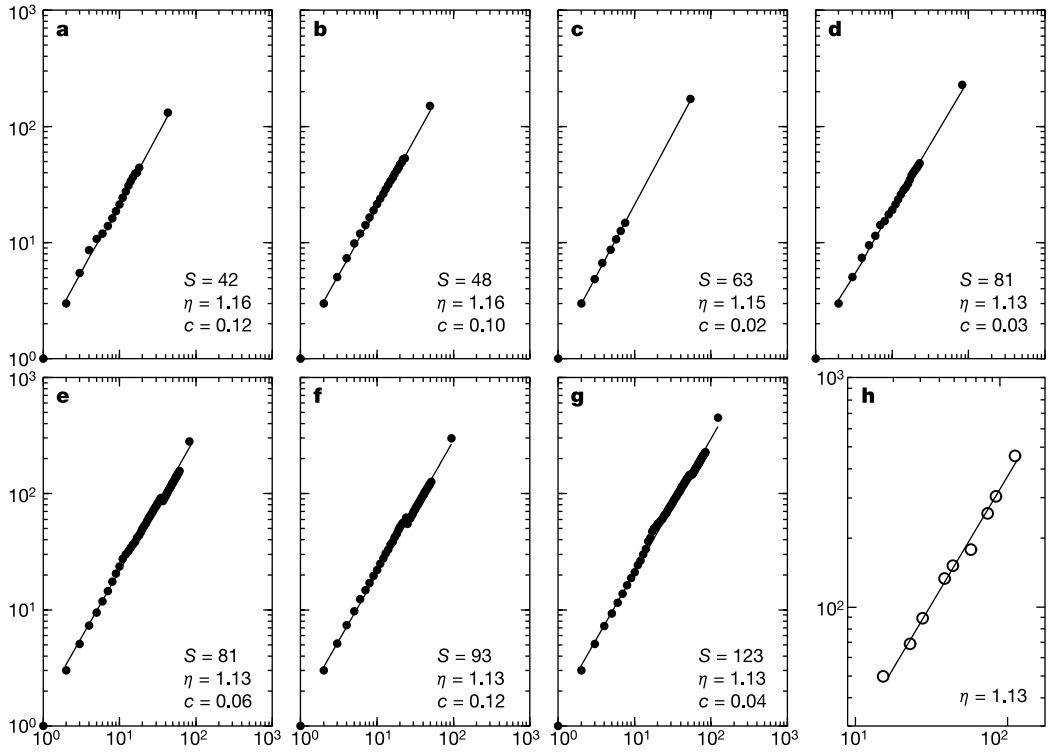

Figure 2 Scaling of C against A. Plot of scaling relations C_i against A_i (see the text and Methods) and the best power-law fit (the error in the value of the exponent η is always 0.03) to the data. **a**, St Martin Island[7]; **b**, St Marks Seagrass[8]; **c**, grassland[9]; **d**, Silwood Park[10]; **e**, Ythan Estuary without parasites[11]; **f**, Little Rock Lake[12]; **g**, Ythan Estuary with parasites[13] (for each web, the number of species S and the connectance c are also reported). **h**, Plot of C_0 against A_0 for a collection of webs[6–15] including those in **a**–**g**; see Methods (note that the scale is different).

Table 1 **Predictions of food web models**

c	η_{Cascade}	η_{Niche}	$\eta^{0}_{\text{Webworld}}$	$\eta^{\infty}_{\text{Webworld}}$	$c^{\infty}_{\text{Webworld}}$
0.005	1.12	1.03	1.83	1.61	0.08
0.01	1.09	1.04	1.51	1.20	0.10
0.05	1.08	1.06	1.33	1.11	0.12
0.1	1.06	1.08	1.22	1.09	0.18
0.3	1.04	1.07	1.18	1.07	0.37
0.5	1.01	1.04	1.05	1.04	0.50

The value of the exponent η (the error is always about 0.02) in different models is shown as a function of the connectance c. In static (Cascade[3] and Niche[24]) models the exponent (η_{Cascade} or η_{Niche}) is determined by a single tuning parameter related to c. In the Webworld model[23], a competition parameter tunes the initial state (characterized by the initial values c and $\eta^{0}_{\text{Webworld}}$). Then the model evolves and reaches an 'asymptotic' state characterized by a smaller exponent $\eta^{\infty}_{\text{Webworld}}$ and by a larger connectance $c^{\infty}_{\text{Webworld}}$ (both efficiency and stability increase; see the text). All webs have 1,000 species initially.

former determine the tree structure related to the efficiency of the webs, and the latter form the loops involved in network robustness. Whereas the different nature of the interactions affects the number of loops[29] (and hence the stability), the structure of the spanning trees seems to be invariant and universal. Correspondingly, although the stability properties are likely to be determined by different evolutionary processes, the efficiency of food webs might be the result of a common organizing principle. □

Methods

To define the minimal spanning tree, we discuss two different approaches. One possibility is considering the spanning tree defined by the collection of the shortest chains from the environment to every species (the number of links in these chains gives the trophic level[1–3] of the species). If several spanning trees are still compatible with this prescription, we consider all of them and then perform an ensemble average (see below). Alternatively, we can select for each species the strongest chain from the environment; that is, the one delivering most resources to the species. We prefer to adopt the former definition to include a larger number of data sets in the analysis and to compare them with the models, which in most cases ignore link strength. However, we note that the chains obtained by the two criteria (minimizing chain lengths and maximizing chain strengths) are related. Generally, the transfer of resources along each link is 'inefficient' (only a small fraction of resources is transferred from prey to predator[1,2]) and hence long chains are likely to be weaker than short ones[1]. This argument is also consistent with the empirical observation[2] that only a fraction $\lambda = 0.1$ (known as the ecological efficiency) of the resources of the species in a trophic level is transferred to predators. However, we stress that our definition of 'weak' and 'strong' links does not necessarily reflect the actual link strength.

To obtain the spanning tree minimizing chain length, we first order the species in levels (labelled by $l = 0,1,\ldots,l_{\max}$). Conventionally, the environment belongs to level $l = 0$. All species preying on species at level l (but not at lower ones) belong to level $l + 1$. We then remove all the 'weak' links pointing from a species at a given level l_1 to a species at a level l_2 lower than or equal to l_1. At this point, if each species is left with only one incoming link, the spanning tree is already obtained (all remaining links are 'strong') and the quantities A_i and C_i are directly computed and plotted. Otherwise, if some species still have more than one incoming link, we consider the ensemble of all possible spanning trees (each defined by a different set of 'strong' links) and compute the quantities A_i and C_i on each of them separately. Finally, for each value of A, the average of the corresponding values of C is computed and plotted as a function of A. This produces the curves shown in Fig. 2a–g. The point (A_0,C_0) is the same for every tree in the ensemble of possible ones. The point (1,1) always occurs as a finite-size effect (it corresponds to the 'leaves', where the tree stops branching) together with the point (2,3) independently of the large-scale behaviour of the scaling relations (see Fig. 1). A power-law exactly crossing both points would then miss all other points, unless the value of the exponent were 2. We therefore always exclude the point (1,1) from the fit to avoid forcing the exponent towards an artificially high value. We finally obtain the composite figure (Fig. 2h) by simply plotting together the points (A_0,C_0) of each of the previous panels plus the three additional webs described in the text (we recall that these points are independent of the specific spanning tree realization). The value of C_0 corresponding to $A_0 = 82$ is an average of the values of Silwood Park and Ythan Estuary without parasites (both webs have 81 trophic species).

Received 25 July 2002; accepted 20 March 2003; doi:10.1038/nature01604.

1. Lawton, J. H. in *Ecological Concepts* (ed. Cherret, J. M.) 43–78 (Blackwell Scientific, Oxford, 1989).
2. Pimm, S. L. *Food Webs* (Chapman & Hall, London, 1982).
3. Cohen, J. E., Briand, F. & Newman, C. M. *Community Food Webs: Data and Theory* Biomathematics 20 (Springer, Berlin, 1990).
4. Strogatz, S. H. Exploring complex networks. *Nature* **410,** 268–276 (2001).
5. Albert, R. & Barabási, A.-L. Statistical mechanics of complex networks. *Rev. Mod. Phys.* **74,** 47–97 (2002).
6. Cohen, J. E. *Ecologists' Co-Operative Web Bank 1.00* (The Rockfeller Univ., New York, 1989).
7. Goldwasser, L. & Roughgarden, J. Construction and analysis of a large Caribbean food web. *Ecology* **74,** 1216–1233 (1993).
8. Christian, R. R. & Luczkovich, J. J. Organizing and understanding a winter's seagrass foodweb network through effective trophic levels. *Ecol. Mod.* **117,** 99–124 (1999).
9. Martinez, N. D., Hawkins, B. A., Dawah, H. A. & Feifarek, B. P. Effects of sampling effort on the characterization of food web structure. *Ecology* **80,** 1044–1055 (1999).
10. Memmott, J., Martinez, N. D. & Cohen, J. E. Predators, parasitoids and pathogens: species richness, trophic generality and body sizes in a natural web. *J. Anim. Ecol.* **69,** 1–15 (2000).
11. Hall, S. J. & Raffaelli, D. Food web patterns: lessons from a species-rich web. *J. Anim. Ecol.* **60,** 823–842 (1991).
12. Martinez, N. D. Artifacts or attributes? Effects of resolution on the Little Rock Lake food web. *Ecol. Monogr.* **61,** 367–392 (1991).
13. Huxham, M., Beaney, S. & Raffaelli, D. Do parasites reduce the chances of triangulation in a real food web? *Oikos* **76,** 284–300 (1996).
14. Polis, G. A. Complex trophic interactions in deserts: an empirical critique of food web theory. *Am. Nat.* **138,** 123–155 (1991).
15. Warren, P. H. Spatial and temporal variation in the structure of a freshwater food web. *Oikos* **55,** 299–311 (1989).
16. Montoya, J. M. & Solé, R. V. Small world patterns in food webs. *J. Theor. Biol.* **214,** 405–412 (2002).
17. Williams, R. J., Berlow, E. L., Dunne, J. A. & Barabási, A.-L. Two degrees of separation in complex food webs. *Proc. Natl Acad. Sci. USA* **99,** 12913–12916 (2002).
18. Camacho, J., Guimerà, R. & Amaral, L. A. N. Robust patterns in food web structure. *Phys. Rev. Lett.* **88,** 228102 (2002).
19. Dunne, J. A., Williams, R. J. & Martinez, N. D. Food-web structure and network theory: the role of connectance and size. *Proc. Natl Acad. Sci. USA* **99,** 12917–12922 (2002).
20. Banavar, J. R., Maritan, A. & Rinaldo, A. Size and form in efficient transportation networks. *Nature* **399,** 130–132 (1999).
21. West, G. B., Brown, J. H. & Enquist, B. J. A general model for the origin of allometric scaling laws in biology. *Science* **276,** 122–126 (1997).
22. West, G. B., Brown, J. H. & Enquist, B. J. The fourth dimension of life: fractal geometry and allometric scaling of organisms. *Science* **284,** 1677–1679 (1999).
23. Caldarelli, G., Higgs, P. G. & McKane, A. J. Modelling coevolution in multispecies communities. *J. Theor. Biol.* **193,** 345–358 (1998).
24. Williams, R. J. & Martinez, N. D. Simple rules yield complex food webs. *Nature* **404,** 180–183 (2000).
25. Rodriguez-Iturbe, I. & Rinaldo, A. *Fractal River Basins: Chance and Self-Organization* (Cambridge Univ. Press, Cambridge, 1996).
26. McMahon, T. A. & Bonner, J. T. *On Size and Life* (Scientific American Library, New York, 1983).
27. Martinez, N. D. Constant connectance in community food webs. *Am. Nat.* **139,** 1208–1218 (1992).
28. Dunne, J. A., Williams, R. J. & Martinez, N. D. Network structure and biodiversity loss in food webs: robustness increases with connectance. *Ecol. Lett.* **5,** 558–567 (2002).
29. Cousins, S. H. Species diversity measurements: choosing the right index. *Trends Ecol. Evol.* **6,** 190–192 (1991).
30. Drossel, B., Higgs, P. G. & McKane, A. J. The influence of predator–prey population dynamics on the long-term evolution of food web structure. *J. Theor. Biol.* **208,** 91–107 (2001).

Acknowledgements We acknowledge support from the FET Open Project IST-2001-33555 COSIN.

Competing interests statement The authors declare that they have no competing financial interests.

Correspondence and requests for materials should be addressed to G.C. (gcalda@pil.phys.uniroma1.it).

Defective membrane repair in dysferlin-deficient muscular dystrophy

Dimple Bansal*, Katsuya Miyake†, Steven S. Vogel‡, Séverine Groh*, Chien-Chang Chen*, Roger Williamson§, Paul L. McNeil† & Kevin P. Campbell*

** Howard Hughes Medical Institute, Department of Physiology and Biophysics and Department of Neurology, University of Iowa Roy J. and Lucille A. Carver College of Medicine, Iowa City, Iowa 52242, USA*
† Department of Cellular Biology and Anatomy, The Medical College of Georgia, Augusta, Georgia 30912, USA
‡ Laboratory of Molecular Physiology, National Institute of Alcohol Abuse and Alcoholism, National Institutes of Health, Rockville, Maryland 20852, USA
§ Department of Obstetrics and Gynecology, University of Iowa College of Medicine, Iowa City, Iowa 52242, USA

Muscular dystrophy includes a diverse group of inherited muscle diseases characterized by wasting and weakness of skeletal muscle[1]. Mutations in dysferlin are linked to two clinically distinct muscle diseases, limb-girdle muscular dystrophy type 2B and Miyoshi myopathy, but the mechanism that leads to